Journal of Power Sources 193 (2009) 890–894

Contents lists available at ScienceDirect

Journal of Power Sources

journal homepage: www.elsevier.com/locate/jpowsour

Short communication

The inhibition of the spongy electrocrystallization of zinc from doped flowing alkaline zincate solutions

Yue-hua Wen[a,*], Jie Cheng[a], Li Zhang[b], Xu Yan[a], Yu-sheng Yang[a,b]

[a] Research Institute of Chemical Defense, Beijing, 100191, China
[b] Beijing Science and Technology University, Beijing, 100191, China

ARTICLE INFO

Article history:
Received 18 February 2009
Received in revised form 20 April 2009
Accepted 22 April 2009
Available online 3 May 2009

Keywords:
Zinc-air flow battery
Zinc electrocrystallization
Spongy zinc
Morphology
Additives

ABSTRACT

The effects of the presence of additives like lead and tungstate ions in flowing alkaline zincate solutions on suppressing spongy zinc electrogrowth are examined. The results show that the two additives with optimal concentrations in flowing electrolytes can suppress spongy zinc initiation and propagation. And, the two additives can bring about more uniform and compact deposits and, thereby, reduce spongy zinc growth. The influence of lead and tungstate ions on the zinc deposition/dissolution is evaluated by cyclic voltammetry. It also shows that the addition of the two additives is largely a blocking action, and the co-deposition of lead and zinc ions may occur. The performance of the zinc-air flow battery with zinc regeneration electrolysis is determined. It shows that by the addition of 0.6 M Na_2WO_4 or 10^{-4} M to 10^{-3} M lead, compact or mixed compact–spongy zinc deposits are created and the favorable charge/discharge performance of the battery is achieved with an energy efficiency of approximately 60%.

1. Introduction

Due to its low equilibrium potential, good reversibility, low cost, high energy density and low toxicity, zinc has a wide variety of applications as a negative electrode material in batteries. The zinc-based batteries have high energy/power densities per unit volume when compared with other alkaline batteries [1,2]. However, during cycling of secondary zinc-based batteries, dendrites formation, shape change, surface passivation and self-discharge of zinc electrodes lead to poor battery performance and gradual capacity loss. So far, many attempts have been undertaken to overcome these difficulties. Although the cycle life and properties of zinc electrodes are improved by incorporating additives in the electrolyte, the problems still remain elusive [3–5]. Recently, two types of novel redox flow battery systems were proposed by us, namely, single flow zinc-nickel battery [6] and zinc-air battery using zinc regeneration electrolysis with propanol oxidation as a counter electrode reaction [7]. In these two secondary batteries, the use of flowing electrolytes provides an effective approach to suppress dendritic growth, shape change and passivation of zinc electrodes [8]. However, spongy zinc deposits are easy to be formed from flowing alkaline zincate solutions. Thus, the performance of batteries is influenced to a significant degree.

Employment of inorganic additives in stationary electrolytes of zinc-alkaline cells is well known. Additives such as CdO [9], Bi_2O_3 [10], Pb_3O_4 [11] have been shown to be beneficial for an enhancement in the performance of zinc-based alkaline cells. At least two mechanisms have been proposed to explain the improved cell performance using these inorganic additives [2]. First, if the additive is present as the reduced metal, it may serve as a substrate that promotes the formation of compact and thin zinc deposits via electro-deposition. Second, the incorporation of metallic deposits in zinc electrodes enhances the electronic conductivity and polarizability of the electrode. For applications in flow zinc-alkaline cells, inorganic additives must firstly be soluble in the electrolytes, and secondly their standard potentials should be higher than the standard potential of zinc.

In this study, the effects of soluble inorganic additives (viz., PbO and Na_2WO_4 [12]) on the electrochemical behavior of zinc in flowing electrolytes are examined by voltammetry, scanning electron microscope (SEM) techniques and charge–discharge measurements. The deposition was carried out in a zinc air battery with zinc regeneration electrolysis [7]. The logical aim of the study is to arrive at a suitable additive and optimize its concentration so that the zinc electrode has minimum spongy growth and good electrochemical behavior with a view to fabricate a secondary zinc-based flow alkaline system.

* Corresponding author at: West Building, 35# Huayuanbei Road, Beijing, 100191, China. Tel.: +86 10 66705840; fax: +86 10 66748574.
E-mail address: wen_yuehua@126.com (Y.-h. Wen).

0378-7753/$ – see front matter © 2009 Elsevier B.V. All rights reserved.
doi:10.1016/j.jpowsour.2009.04.047

2. Experimental

2.1. Cyclic voltammetry

A three electrode cell assembly was used with a Hg/HgO electrode as the reference electrode, a large graphite sheet as the counter electrode and a nickel electrode as the working electrode. The working electrode was a disc electrode of nickel (99.99%, Johnson Matthey Chemicals, Beijing, China) which was embedded in an epoxy holder so as to expose a free surface area of 0.196 cm^2. Prior to each experiment, the nickel electrode was polished with emery paper 1000 grade, followed by ultrasonic cleaning in distilled water. Two base electrolytes were employed, namely, a 6 M KOH solution with 0.4 M ZnO and a 6 M KOH solution with 0.4 M ZnO in presence of additives of different concentrations. The voltammograms were measured by the CHI1100A electrochemical station (CH Corporation, USA) at room temperature.

2.2. Charge–discharge behavior of experimental zinc-air cells with zinc regeneration electrolysis

A newly treated nickel sheet was employed as the negative substrate electrode. A sintered nickel electrode (0.31 mm thick) was employed as the positive electrode. The experimental cell with an active area of 5.5 cm^2 was made as described in the literature [7]. The two half-cell electrolytes were separated by a sheet of Nafion 115 cation-exchange membrane to fabricate the electrolysis cell. 35 mL of 0.4 M ZnO in 6 M KOH solution containing additives of different concentrations was employed as the cathodic electrolyte and 35 mL of 0.5 M propanol in 6 M KOH solution was employed as the anodic electrolyte. Two Xishan pumps (China) were used to pump each half-cell electrolyte through the corresponding half-cell cavity, where the electrolysis reactions occurred. A current density of 20 mA cm^{-2} was applied to the cell for 210 min to study the surface morphology of the zinc deposits over the nickel electrode. Then the surface morphologies of zinc deposits were examined by a scanning electron microscope (SEM, Cambridge S-360). The treatment of zinc deposits was described in the literature [8].

At the end of charge, the sintered nickel positive electrode was substituted with an air electrode (Boxin Shanghai Battery Corp., China). And then, the air electrode was combined with the deposited zinc electrode in the flowing electrolyte to form another cell to deliver energy. The discharge process of constant-current was also carried out at the current density of 20 mA cm^{-2}.The performance of test cells was evaluated by a battery test system CT2000A (Jinnuo Wuhan Corp., China) at room temperature.

3. Results and discussion

3.1. Cyclic voltammetry

Fig. 1 shows voltammograms with the first scan cycle on the nickel electrode in 6 M KOH containing 1 M ZnO in the presence of additives. It can be seen that a cathodic peak at about −1.45 V (vs.Hg/HgO) and a corresponding anodic peak at about −1.2 V (vs.Hg/HgO) are obtained in an additive-free solution. In Fig. 1A, with increasing lead ion concentration, the cathodic peak gradually cannot be observed. At lead ion concentrations higher than 10^{-4} M, the cathodic current profiles on the negative scan and on the reverse scan are almost overlapped. Correspondingly, with increasing the lead ion concentration, the anodic peak is shifted towards a more positive value and becomes wider with a continuous decrease in the peak current. It is rather significant at 5×10^{-3} M lead. Further, when the lead ion concentration reaches 5×10^{-3} M, the cathodic current profiles on the negative scan and on the reverse scan are separated and another small anodic peak at about −0.63 V (vs.Hg/HgO) appears. This new anodic peak might be associated with the dissolution of lead. It suggests that the zinc deposition is inhibited to a certain degree owing to the addition of lead ions and the co-deposition of lead and zinc ions may occur.

Comparatively, the addition of tungstate ions in the electrolytes causes the cathodic peak and the anodic peak to be lowered as shown in Fig. 1B. And, the cathodic current value is not dependent on the tungstate concentration. In contrast, the anodic peak current decreases progressively with an increase in the tungstate concentration. And, the potential of the cathodic peak is shifted towards a more negative value by about 20 mV. It indicates that the zinc deposition/dissolution is inhibited to a certain degree, which may slow the rate of zinc deposition/dissolution during electrode charging/discharging and, thereby, mitigate the spongy zinc growth. However, too large polarization would be detrimental for the zinc deposition and lead to a reduction in the charge efficiency of the cell.

3.2. Charge–discharge behavior of experimental zinc-air battery with zinc regeneration electrolysis

The cell was charged at the current density of 20 mA cm^{-2} for 210 min, and discharged at the same current density to a cut-off

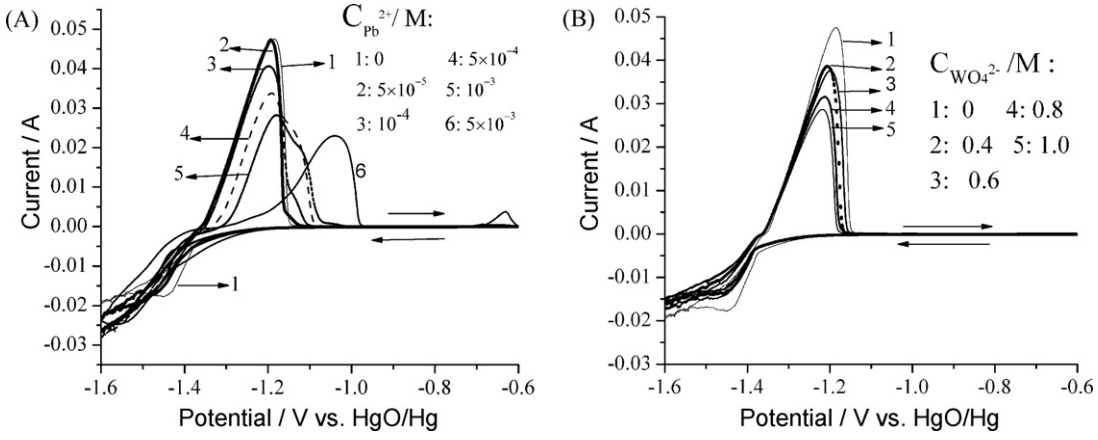

Fig. 1. Cyclic voltammograms for nickel electrodes in 6 M KOH containing 0.4 M ZnO and additives with various concentrations on the first cycle: (A) lead ions and (B) tungstate ions. Scan rate: 10 mV s^{-1}.

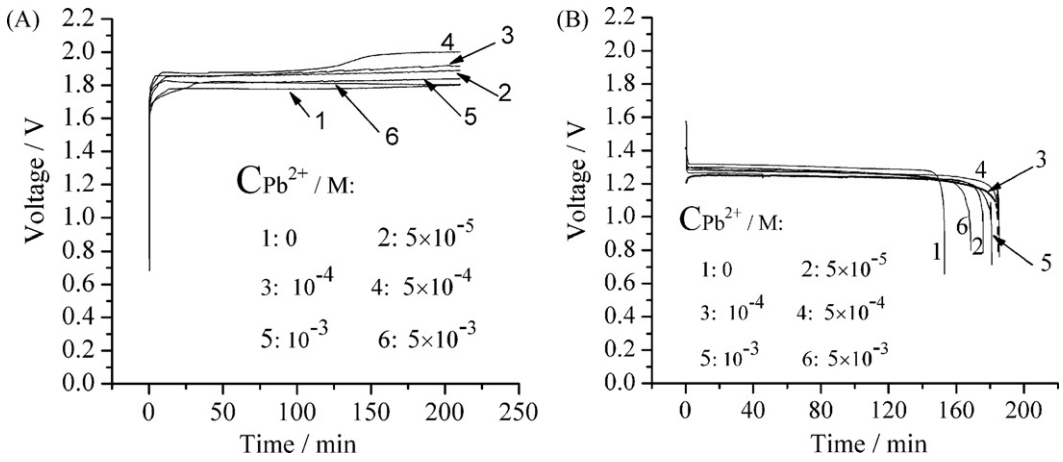

Fig. 2. Constant–current charge (A) and discharge (B) curves of the zinc-air flow battery as a function of the lead concentration in the electrolyte. Current density: 20 mA cm^{-2}.

voltage of 0.8 V. The voltage–time curves for the charging and discharging as a function of lead ion concentration are illustrated in Fig. 2. As the concentration of lead ions is increased to 5×10^{-4} M, charge polarization of the cell increases, and its charge plateau voltage rises gradually. A further increase of the lead ion concentration conversely causes a little decrease in the charge voltage. Correspondingly, the discharge plateau voltage is slightly lower than that with no additives. However, the discharge time of the cell is continuously prolonged with the increase of lead ion concentration. The longest discharge time is obtained at 5×10^{-4} M and 10^{-4} M lead. In combination with the voltage efficiencies, the energy efficiency of up to 58% can be obtained at the lead concentration ranging from 10^{-4} M to 10^{-3} M. This may be attributed to a change in zinc deposit morphology.

The voltage–time curves for the charging and discharging as a function of tungstate concentration are presented in Fig. 3. It can be seen that compared with no additives, the charging voltage of test cells is raised to varying degrees. Correspondingly, the discharging voltage just decreases a little. But, the discharge time is extended obviously. The longest discharge time is achieved at 0.6 M Na_2WO_4. This reflects the suppression of spongy zinc growth and the formation of compact zinc deposition. Thus, the cell exhibits the best charge/discharge performance at 0.6 M Na_2WO_4. The coulombic and energy efficiencies reach 91% and 59%, respectively.

3.3. Studies on surface morphology

SEM graphs of zinc deposits after the 210-min charge, are given in Figs. 4 and 5. It can be seen that without additives in the electrolyte, the zinc is deposited as an irregular sponge to give a three-dimensional structure (Fig. 4A). The effects of adding lead ions with different concentrations, are shown in Fig. 3B–D. The formation of spongy deposits is effectively inhibited by the addition of only 5×10^{-5} M lead ions. At 5×10^{-4} M lead, some pits and heaves appear on the compact zinc deposit. At 10^{-3} M lead, the behavior is indicative of mixed spongy and compact zinc growth. It is expected that if the lead ion concentration is increased further, spongy zinc deposits would be formed again. It suggests that when zinc deposits exhibit mixed compact and spongy morphologies, the contact resistance between zinc deposits and substrate electrodes is not only low but also the electrode activity is relatively high. Correspondingly, the energy efficiency obtained at 10^{-3} M lead is the same high level as that at 5×10^{-4} M or 10^{-4} M lead due to the formation of compact zinc deposits.

The effects of adding tungstate ions after the 210-min charge are shown in Fig. 5. As can be clearly seen, a compact deposit is observed when the tungstate concentration reaches 0.6 M. Otherwise, spongy zinc deposits are formed again to varying degrees. Thus, the best charge/discharge performance of the battery is achieved at 0.6 M Na_2WO_4. This is distinguished from the addi-

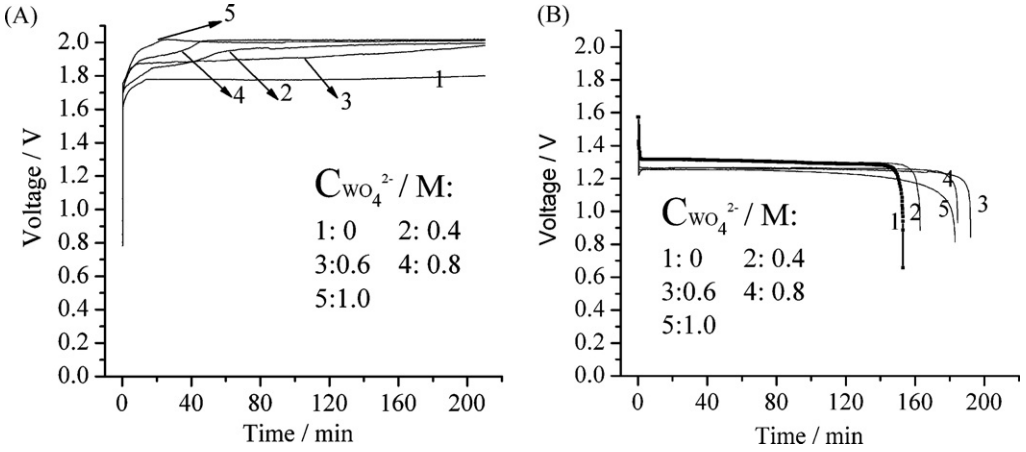

Fig. 3. Constant–current charge (A) and discharge (B) curves of the zinc-air flow battery as a function of the tungstate concentration in the electrolyte. Current density: 20 mA cm^{-2}.

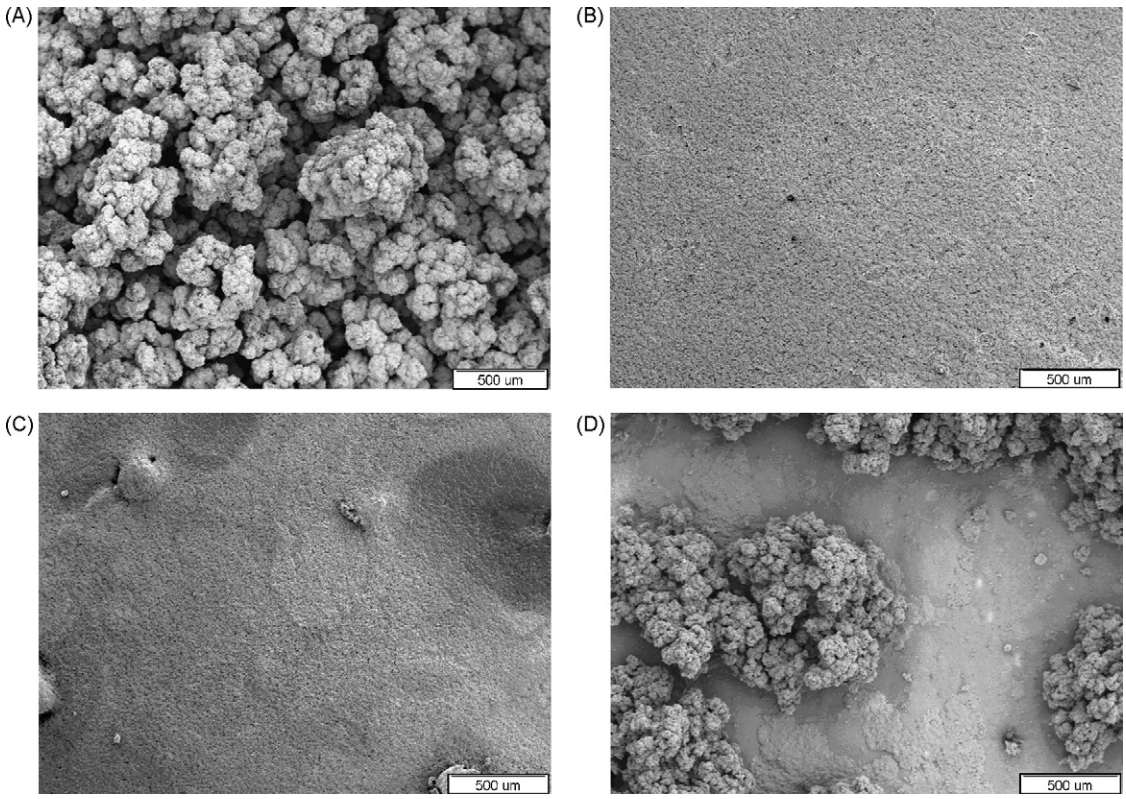

Fig. 4. Electron micrographs of the surface morphology of zinc deposites in the presence of lead ions with different concentrations: (A) 0 M, (B) 5×10^{-5} M, (C) 5×10^{-4} M and (D) 10^{-3} M.

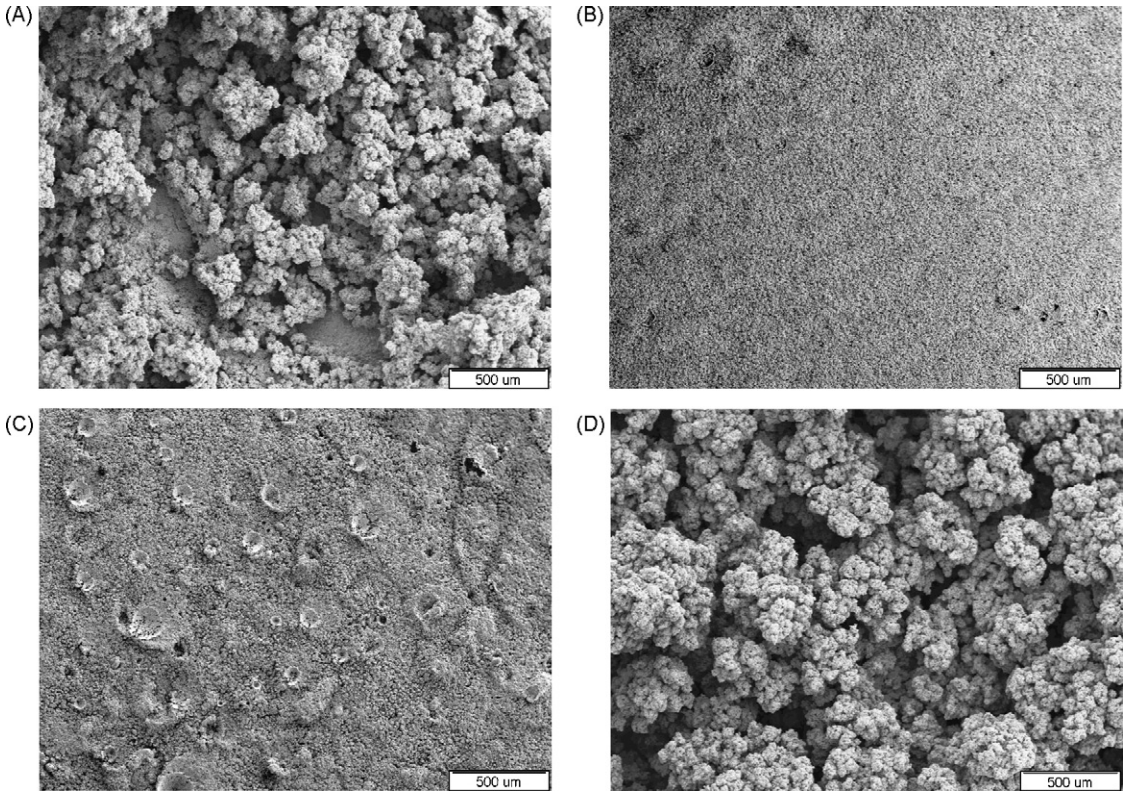

Fig. 5. Electron micrographs of the surface morphology of zinc deposites in the presence of tungstate ions with different concentrations: (A) 0.4 M, (B) 0.6 M, (C) 0.8 M and (D) 1.0 M.

tion of lead ions which is possibly attributable to the different mechanisms in inhibiting the spongy zinc growth as shown in the voltammograms.

4. Conclusion

The effectiveness of lead and tungstate ions as inhibitors of zinc spongy growth in flowing alkaline zincate solutions has been examined. The addition of the two additives with optimal concentrations to the flowing electrolytes is found to effectively suppress spongy zinc initiation and propagation. The influence of the lead and tungstate ions on zinc deposition is indicated as being largely a blocking action. Also, the addition of lead ions is effective in preventing the spongy zinc growth by co-deposition. The performance of zinc-air flow battery with zinc regeneration electrolysis in the presence of the two additives in electrolytes was determined. It shows that by the addition of 0.6 M Na_2WO_4 or 10^{-4} M to 10^{-3} M lead, compact or mixed compact–spongy zinc deposits are created and the favorable charge/discharge performance of the battery is achieved with an energy efficiency of approximately 60%.

Acknowledgement

This work is financed by NSFC, the National Natural Science Foundation of China (No. 50804050 and No. 20573135).

References

[1] J.X. Yu, H.X. Yang, X.P. Ai, J. Power Sources 103 (2001) 93.
[2] F.R. McLarnon, E.J. Cairns, J. Electrochem. Soc. 138 (1991) 645.
[3] C.W. Lee, K. Sathiyanarayanan, S.W. Eom, J. Power Sources 159 (2006) 1474.
[4] R. Shivkumar, G.P. Kalaignan, T. Vasudevan, J. Power Sources 55 (1995) 53.
[5] R. Shivkumar, G.P. Kalaignan, T. Vasudevan, J. Power Sources 75 (1998) 90.
[6] J. Cheng, L. Zhang, Y.S. Yang, Y.H. Wen, Electrochem. Commun. 9 (2007) 2639.
[7] Y.H. Wen, J. Cheng, S.Q. Ning, Y.S. Yang, J. Power Sources 188 (2009) 301.
[8] L. Zhang, J. Cheng, Y.S. Yang, J. Power Sources 179 (2008) 381.
[9] R. Renuka, S. Ramamurthy, L. Srinivasan, J. Power Sources 89 (2000) 70.
[10] J. McBreen, E. Gannon, J. Power Sources 15 (1985) 169.
[11] J.W. Diggle, A. Damjanovic, J. Electrochem. Soc. 119 (1972) 1649.
[12] H.L. Zeng, Z.T. Wu, Electroplating Arts and Crafts Manual, Mechanical Industry Press, Beijing, 1997.